

***Ab initio* MO Calculations on the Structure and Raman and Infrared Spectra of $[\text{Al}_4\text{O}_2\text{Cl}_{10}]^{2-}$ Oxide in Chloroaluminate Melts**

Rolf W. Berg

Department of Chemistry, Technical University of Denmark, Kemitorvet, Building 207, DK-2800 Lyngby, Denmark

Reprint requests to Prof. R. W. B.; Fax: +45 45 88 31 36; E-mail: rwb@kemi.dtu.dk

Z. Naturforsch. **62a**, 157–168 (2007); received February 6, 2007

Presented at the *EUChem Conference on Molten Salts and Ionic Liquids, Hammamet, Tunisia, September 16–22, 2006.*

The oxide complexation chemistry in molten tetrachloroaluminate salts and ionic liquids is discussed with respect to what possible structures may be formed in addition to $[\text{AlCl}_4]^-$: $[\text{Al}_2\text{OCl}_6]^{2-}$, $[\text{Al}_3\text{OCl}_8]^-$, $[\text{Al}_2\text{O}_2\text{Cl}_4]^{2-}$, $[\text{Al}_3\text{O}_2\text{Cl}_6]^-$ and $[\text{Al}_4\text{O}_2\text{Cl}_{10}]^{2-}$. *Ab initio* molecular orbital calculations are carried out on these various aluminium chloride and oxochloride ions, in assumed isolated gaseous free ionic state, by use of the Gaussian 03W program at the restricted Hartree-Fock (HF) level and with the 6-31+G(d,p) basis set. Without any pre-assumed symmetries and with tight optimization convergence criteria and by using the modified GDIIS algorithm, the model calculations generally converge. The structures and their binding energies are presented. The expected geometries are supported, with one exception perhaps being the $[\text{Al}_2\text{OCl}_6]^{2-}$ ion, that gave a linear Al-O-Al bonding system of staggered AlCl_3 -groups (approximate D_{3d} symmetry), in analogy to the linear Al-O-Al geometry of the analogous $[\text{Al}_2\text{OF}_6]^{2-}$ ion, found previously. The calculations include determination of the vibrational harmonic normal modes and the infrared and Raman spectra (vibrational band wavenumbers and intensities), without any empiric adjustments of the harmonic force constants, using constants directly predicted from the Gaussian 03W program. Previously obtained IR absorption and Raman scattering spectra of melts are assigned, by comparing to the *ab initio* quantum mechanical vibrational analysis results. It is concluded that the small oxide content commonly found in basic and neutral tetrachloroaluminate melts, most probably consists of $[\text{Al}_4\text{O}_2\text{Cl}_{10}]^{2-}$ ions, and the vibrational spectra are given.

Key words: Raman and Infrared Spectroscopy; IR; Hartree-Fock; Tetrachloroaluminate; Ionic Liquid; Molten Salt.

1. Introduction

Ab initio molecular orbital (MO) calculations have recently become quite efficient to predict chemical structures and vibrational [Raman scattering and infrared (IR) absorption and emission] spectra, e. g. by means of the Gaussian 03W program [1]. Molten inorganic or organic chloroaluminates are of considerable interest because of their use as effective media for unusual redox and coordination chemistry, and because of their composition-dependent Lewis acidities. We here report a study to use the *ab initio* calculation approach to understand better certain features of these melts, as explained in the following.

The vibrational spectra of inorganic chloroaluminate melts (metal chloride/aluminium chloride molten

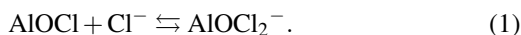
mixtures) are well established for the alkali and alkaline-earth chloroaluminates, see e. g. [2–20] and references therein. Also chloroaluminate melts or ionic liquids with various organic anions have been studied by IR and Raman spectroscopy, see e. g. [21–26].

The problem of oxide contamination of these hygroscopic chloroaluminate melts has been of some concern [4–11, 20]. Small amounts of oxide impurities in these melts may have pronounced effects on the behaviour of other solute species of interest, a fact of importance, e. g. during plating of metals from solutions. The presence of traces of oxide in these melts is difficult to avoid, and it is difficult to detect the presence of the oxides [27].

Advanced methods to clean the melts have been developed, e. g. by treatment with phosgene [28–30] or

carbon tetrachloride [31, 32]. The removal of oxide from these melts is based on the reaction of COCl_2 or CCl_4 with oxide ions in the melts. The complete conversion of the oxide-containing chlorides to clean melts has been proven by different techniques (UV-visible and IR spectroscopy), and the oxide content in chloroaluminate melts has even been detected by ^{17}O NMR spectroscopy [33] and Karl Fischer titration [34]. Also fractionated recrystallization has been used as an effective way of cleaning tetrachloroaluminate media [4].

There has been some speculation and confusion on the speciation of the oxide impurities, see e. g. the summary given in [4]. The reaction of O^{2-} ions with Al^{3+} ions in alkali halide environment was modelled, trying to understand the energetics [35]. It is now generally agreed that hardly any free O^{2-} ions can be present. Oxochloroaluminate species like “ AlOCl ” or “ AlOCl_2^- ” have been postulated [5, 36–43], occurring in low concentrations, depending on the chloride concentration according to the mutual equilibrium



Cryoscopic [4] and potentiometric [10, 11] measurements have been interpreted to show that species like $(\text{AlOCl})_n \cdot (\text{AlCl}_4^-)_m$ with $n = 2$ and $m = 1$ or 2 occur in the melts.

In the solid phase, the salts $[(\text{C}_6\text{H}_6)(\text{C}_6\text{Me}_6)\text{Cr}][\text{Al}_3\text{Cl}_8\text{O}] \cdot 0.5\text{C}_6\text{H}_6$ and $[(\text{C}_6\text{Me}_6)_2\text{Nb}_2\text{Cl}_4][\text{Al}_4\text{Cl}_{10}\text{O}_2] \cdot 2\text{CH}_2\text{Cl}_2$, obtained from Friedel-Crafts reactions, and $\text{Ag}_2[\text{Al}_4\text{O}_2\text{Cl}_{10}]$ have been isolated and had their crystal structures solved by single crystal X-ray diffraction methods [44, 45]. The former salt was found to contain $[\text{Al}_3\text{OCl}_8]^-$ ions (I) and the next two salts contained centro-symmetric $[\text{Al}_4\text{O}_2\text{Cl}_{10}]^{2-}$ ions (II). The best characterized salt, $\text{Ag}_2[\text{Al}_4\text{O}_2\text{Cl}_{10}]$, was crystallized from $\text{AgCl}/\text{AlCl}_3$ reaction mixtures when traces of water were present; the deliberate use of the theoretical amount of $\text{AlCl}_3 \cdot 6\text{H}_2\text{O}$ gave a quantitative yield [45].

The idea of using vibrational spectroscopy as a possible way to determine the oxide level has been applied quite extensively, as shown for melts with deliberately added oxide impurities [8, 14–18]. Mamantov et al. [41, 46] have reported a method for determining oxide impurities in molten chloroaluminates based on infrared measurements. IR emittance and external reflectance spectra were obtained of several AlCl_3 - NaCl_{sat} melt samples using a diamond-windowed cell;

peak heights at 801 and 680 cm^{-1} were correlated to oxide concentration as determined by potentiometric analysis [42].

Einarsrud [15], e. g., recorded FT-IR reflection spectra of molten $\text{Na}[\text{AlCl}_4]$ containing AlOCl and even a metastable melt with the composition “ $\text{NaAl}_2\text{OCl}_5$ ”, prepared from NaCl , AlCl_3 and $\text{AlCl}_3 \cdot 6\text{H}_2\text{O}$ at a molar ratio of 6 : 11 : 1 in a large thick-walled quartz ampoule that was sealed and heated to melting at 120 °C. She obtained a clear and highly viscous melt that, after 2–3 d at room temperature, started to crystallize. Formed HCl was frozen out or removed under vacuum. Chemical analyses of the “ $\text{NaAl}_2\text{OCl}_5$ ” product gave: Al 19.4(19.9), O 6.00(5.9), Cl 66.1(65.6), H < 0.02% by weight [15]; values in parentheses are calculated, assuming the solid to consist as “ $\text{NaAl}_2\text{OCl}_5$ ” [14–18].

The complex ion $[\text{Al}_4\text{O}_2\text{Cl}_{10}]^{2-}$ was predicted by MNDO/3 MOPAC calculations to be stable when isolated, and the calculated IR spectrum fitted the observed IR spectrum [18]. Three different reaction products, obtained on addition of AlCl_3 to $\text{NaAl}_2\text{OCl}_5$, were examined and the predicted spectrum of the reaction products was compared with the IR spectrum of the reaction mixtures. Also, presumably $\text{Na}[\text{Al}_3\text{OCl}_8]$ has been measured in the region IR [12].

Obviously we may learn something on the oxochloroaluminates by comparing with the analogous fluoride systems. The well known Hall-Héroult process, used world-wide for the production of aluminium metal, takes advantage of the significant solubility of alumina (Al_2O_3) in molten fluorides (mostly cryolite Na_3AlF_6) at high temperatures, but the species formed are not well established, see e. g. the discussion in [47–49]. The determination of the oxide content is an important industrial issue, because efficient operation of the electrolysis cells requires the alumina content to be kept at least at a few weight-% [50]. According to cryoscopic studies [51–54], aluminum oxofluoride complex molecular ions rather than free oxide ions are formed when alumina and other oxides are dissolved in molten cryolite. Probably $[\text{Al}_2\text{OF}_6]^{2-}$ is formed in dilute solutions, and perhaps $[\text{Al}_2\text{O}_2\text{F}_4]^{2-}$ ions in more concentrated solutions [55]. The existence of the same species and also $[\text{Al}_3\text{O}_3\text{F}_6]^{3-}$ (rings) in MF- AlF_3 - Al_2O_3 (M = Li, Na, K) melts was deduced by Danek et al. [56], based on the LECO TC-436 nitrogen/oxygen chemical analysis technique in conjunction with carbothermal reduction. Complexes with oxide bridges were required to account for the experimental results

[47, 50, 53, 57]. Many attempts have been made to identify the nature of the complexes by various techniques, among these Raman spectroscopy [58]. Raman bands at about 200 and 510 cm^{-1} were assigned to bridged oxide species [58–60]. Difference methods were used to subtract the broad Raman spectrum of the cryolite solvent at 1020 °C from the Raman spectrum of the mixtures to reveal the peaks assigned to solute species of the type $[\text{Al}_2\text{OF}_6]^{2-}$ and $[\text{Al}_2\text{O}_2\text{F}_4]^{2-}$. The observation of these bands was hampered by low intensity of the oxide bands, in part because of the low solubility of alumina, and in part because of severe overlap with other bands in the cryolite melts. For instance at 1020 °C, the main 555 cm^{-1} band in molten cryolite (presumably due to $[\text{AlF}_5]^{2-}$ [59–62]) has a full width at half height of about 100 cm^{-1} , that makes it difficult to observe the presence of oxide species. At much lower temperatures, $[\text{Al}_2\text{OF}_6]^{2-}$ ions have been found in eutectic LiF/NaF/KF melts (FLiNaK at approximately 500 °C), and trapped in isolated state in solidified FLiNaK at ~ 25 °C [48]. The assignment of harmonic vibrational bands, observed in Raman and IR spectra, to $[\text{Al}_2\text{OF}_6]^{2-}$ ions has been done, based on *ab initio* molecular orbital calculations of IR and Raman vibrational frequencies and intensities performed at the Restricted Hartree-Fock level (RHF) and the 6-31+G* basis set, by means of the Gaussian-92 without any pre-assumed symmetry and with tight convergence criteria [63]. The geometry of $[\text{Al}_2\text{OF}_6]^{2-}$ converged to give a linear Al-O-Al bonding system of approximate D_{3d} symmetry. Similar results for the structure and the IR spectrum had previously also been found in quantum mechanical calculations with triple zeta plus polarization (TZP) basis sets under the generalized gradient approximation (GGA), using Becke and Lee-Yang-Parr correlation and exchange functionals (BLYP) without any fixed symmetry [64].

In the present paper the following ions were studied by *ab initio* calculations: $[\text{AlCl}_4]^-$, $[\text{Al}_2\text{OCl}_6]^{2-}$, $[\text{Al}_3\text{OCl}_8]^-$, $[\text{Al}_2\text{O}_2\text{Cl}_4]^{2-}$, $[\text{Al}_3\text{O}_2\text{Cl}_6]^-$ and $[\text{Al}_4\text{O}_2\text{Cl}_{10}]^{2-}$.

2. Methods, Computational Details and Experimental

2.1. MO Calculations

Molecular orbital (MO) calculations were performed with the Gaussian 03W [1] program on an ordinary office 3 GHz personal computer equipped with

a Pentium R4 processor and 504 MB of RAM and operated under Windows™ XP. The total conformational energy was minimized by use of the restricted Hartree-Fock or DFT/B3LYP procedures. The basis sets used were the split valence basis sets 6-31+G(d,p) with Pople's polarization functions augmented with diffuse orbitals and the modified GDIIS algorithm and with tight optimization convergence criteria [1]. The ions were in assumed gaseous free ionic state and without any pre-assumed symmetries. The vibrational frequencies and the eigenvectors for each normal mode were displayed on the computer screen and identified according to which motions dominated.

2.2. Sample Preparation

We attempted to make a sample of $\text{Ag}_2[\text{Al}_4\text{O}_2\text{Cl}_{10}]$ in the following way: ~ 12 mmol of AgCl and ~ 22 mmol of AlCl_3 were added into a ~ 300 mL long-stemmed ampoule in a dry glove box. It was taken out, ~ 2 mmol of $\text{AlCl}_3 \cdot 6\text{H}_2\text{O}$ were quickly added and the ampoule was sealed under vacuum. Theoretically, from these chemicals – if pure – one may expect the formation of 6 mmol of $\text{Ag}_2[\text{Al}_4\text{O}_2\text{Cl}_{10}]$ and 24 mmol of HCl. Care was and must be taken to avoid accidents. The ampoule was heated to about 200 °C over night in a rocking furnace. An overpressure of about 5 bar of HCl gas was created inside the ampoule. A liquid with a white precipitate was formed (probably a mixture of AgAlCl_4 , AgAl_2Cl_7 , $\text{Ag}_2[\text{Al}_4\text{O}_2\text{Cl}_{10}]$, and solid AlOCl). The formed HCl gas was condensed in the stem (by dipping in liquid nitrogen) and separated with a torch (and the stem broken to avoid explosion). The ampoule was opened in the glove box and the remaining HCl gas pumped off at a slightly elevated temperature.

2.3. Raman Spectroscopy

The use of visible laser light (green, 514.5 nm, or red, 784 nm) to record a Raman spectrum of the prepared sample resulted only in strong fluorescence with our dispersive spectrographs. But it was possible to obtain FT spectra using a Bruker IF S66 FRA-106 Fourier-Transform spectrometer with a Raman attachment. The exciting source was a 1064 nm near-infrared Nd-YAG laser with a nominal power of 100 mW. The scattered light was filtered and collected at a liquid N₂-cooled Ge-diode detector, giving a spectral resolution of approximately 2 cm^{-1} between individual pixels.

Methods/ basis set	Calcd. energy A.U. (Ha)	Bond length calcd. or exptl. (Å)	Modes (wavenumbers / cm^{-1})				Ref.
			$\nu_2(\text{E})$	$\nu_4(\text{T}_2)$	$\nu_1(\text{A}_1)$	$\nu_3(\text{T}_2)$	
HF/3-21G*	-2070.20141	2.23	110	162	297	431	[65]
HF/6-31G*	-2080.23047	2.170	121	192	353	510	[65]
SCF/6-31G*		2.17	121	188	353	511	[66]
HF/6-31G*	-2080.230472	2.17	121.1	187.6	353.1	511.4	[26, 67]
RHF/6-31G*	-2080.23047167		121	188	353	511	[68]
RHF-SCF		2.156	124	192	356	519	[69]
B3LYP		2.168	114	179	336	498	[69]
RHF/6-31+G(d,p)	-2080.23458675	2.17	121	186	353	507	this work
RB3LYP/6-11++G(d,p)	-2083.76111646	2.17	112	174	333	484	this work
Experimental			121	186	351	490	[19]
Experimental			119	182	346	488, 475	[2, 6]
Experimental Na $[\text{AlCl}_4]$ at 20 °C		2.13 ± 0.02					[70, 71]

Table 1. *Ab initio* MO calculations on $[\text{AlCl}_4]^-$ in the gas phase and experimental data.

More than 400 scans were collected in a range from 3500 cm^{-1} (Stokes) to -1000 cm^{-1} (anti-Stokes), at approximately $23 \text{ }^\circ\text{C}$ directly on the ampoule. The resulting spectra were averaged and not corrected for the small changes in instrument response.

3. Results and Discussion

3.1. Tetrachloroaluminate

For purposes of comparison and to make sure that the available Gaussian 03W program [1] performed reasonably well (at the restricted Hartree-Fock level using the 6-31+G* basis set without any pre-assumed symmetry) we have successfully reoptimized the structure and calculated vibrational spectra of the $[\text{AlCl}_4]^-$ ion. We were clearly able to reproduce previous theoretical results [26, 65–69], as shown in Table 1. Experimental data for $[\text{AlCl}_4]^-$ have been given many times in the literature and some representative results are included [2, 6, 19, 70, 71]. The ratio between an experimental and a calculated value is referred to as a scaling factor. Of particular interest it was seen – in other *ab initio* quantum chemical studies of $[\text{MCl}_4]^-$ anions –, that near unit scaling factors were found (of ca. 0.96–0.97) for the HF/6-31G* basis sets, see e. g. [66–69], meaning that the calculated data are close to the experiments. The need for scaling is due to the deficiencies in the models (neglect of correlation energy, use of inferior basis sets, perturbation from counter ions and experimental inaccuracies will cause certain deviations). Nevertheless the errors are small enough to make a reliable structure calculation and assignment of band modes possible. We conclude that the $[\text{AlCl}_4]^-$ ion can be modelled reasonably accurately at the HF/6-31G* and higher levels.

3.2. $[\text{Al}_4\text{O}_2\text{Cl}_{10}]^{2-}$

Next we decided to perform a similar type of *ab initio* calculations on the $[\text{Al}_4\text{O}_2\text{Cl}_{10}]^{2-}$ ion. Since the ion would perhaps adopt two optimized structures, a centro-symmetric one (point group C_i) and one containing a mirror plane of symmetry (point group C_s), we determined two optimized structures, one approximately centro-symmetric (called C_i) and one containing approximately a symmetry mirror plane (called C_s), see Figure 1. The results of the geometric optimizations are given in Table 2, together with experimental geometry data. The energies of the ions were about the same (see Table 2), so most likely both conformations would coexist in a melt at elevated temperatures. The energy for C_i was slightly lower than for C_s , so the C_i should be considered the most stable conformation.

By comparing the geometry values calculated for the equilibrium conformation C_i and the values found from X-ray structure solutions (Table 2), a general satisfactory accordance was found. The overestimation of the Al-Cl bond lengths (0.02–0.06 Å) should be noted, which also was found previously by the MNDO/3 MOPAC calculations on the C_i $[\text{Al}_4\text{O}_2\text{Cl}_{10}]^{2-}$ ion [18]. In conclusion, the modelling

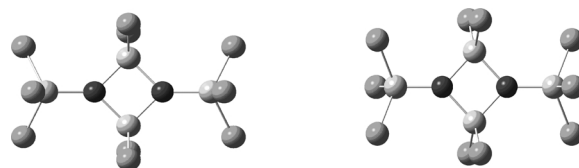
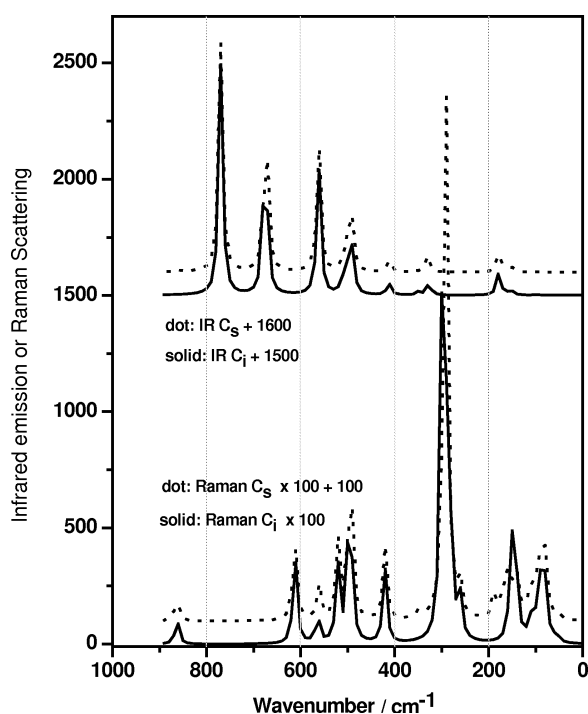


Fig. 1. Optimized geometries of the $[\text{Al}_4\text{O}_2\text{Cl}_{10}]^{2-}$ ion. The left one has an approximate vertical mirror plane (point group symmetry C_s) and the right one has an approximate symmetry centre (point group C_i).

	Calculated approximate		Experimental	
	C_s mirror-symmetry	C_i centro-symmetry	[44] ^a	[45] ^b
Energy calcd. / A.U. ^c	-5723.39782443	-5723.39800295		
<i>Distance / Å; Angles / Degrees^d:</i>				
Al1-O	1.805	1.8061	1.74	1.759
Al1-Cl	2.1697	2.169	2.11	2.127
	2.1702	2.1704	2.12	2.128
	2.1702	2.1704	2.13	2.134
	2.1702	2.1704	2.13	2.134
Al2-O	1.8353	1.8351	1.79	1.798
Al2-Cl	1.8354	1.8351	1.79	1.804
	2.1394	2.1418	2.07	2.105
	2.1439	2.1418	2.09	2.110
	2.1439	2.1418	2.09	2.110
Cl-Al1-Cl	109.277	109.262		108.7
	109.29	109.266		110.4
	110.461	110.44		112.1
Cl-Al1-O	108.578	108.341		110.4
	108.601	108.342		109.6
	110.623	111.173		110.4
Al1-O-Al2	132.983	132.778	130.7	127.8
	133.014	132.782	133.8	138.3
Al2-O-Al2	93.785	94.012	94.0	93.8
O-Al2-Cl	113.36	112.261		114.0
	114.77	115.968		115.0
O-Al2-O	85.9145	85.9876		86.2
Cl-Al2-Cl	112.27	112.12		112.6

Table 2. Optimized geometric structures of the $[\text{Al}_4\text{O}_2\text{Cl}_{10}]^{2-}$ ion as determined by Gaussian-03W DFT RB3LYP/6-31+G(d,p) energy minimization and by X-ray structure determinations in [44, 45].

^a In the salt $[(\text{C}_6\text{Me}_6)_2\text{Nb}_2\text{Cl}_4][\text{Al}_4\text{Cl}_{10}\text{O}_2] \cdot 2\text{CH}_2\text{Cl}_2$ [44]. ^b In the salt $\text{Ag}_2[\text{Al}_4\text{O}_2\text{Cl}_{10}]$ [45]. ^c Hartree. ^d Al1 denotes the aluminium that only is coordinated to one oxygen atom, and Al2 is the one coordinated to two oxygen atoms.



seems to be quite reasonable, taking the approximations into account.

The IR and Raman spectra calculated for the C_i and C_s ions are shown in Fig. 2, and the predicted band

← Fig. 2. IR (top) and Raman spectra (bottom) of $[\text{Al}_4\text{O}_2\text{Cl}_{10}]^{2-}$ ions calculated in this work by RHF/6-31+G(d,p) Gaussian modelling. Upper curves (IR) were arbitrarily shifted by addition of 1500 or 1600, lower curves (Raman) were arbitrarily multiplied by 100 and one shifted by addition of 100.

positions and intensity signals are given in Table 3. It is obvious that the positions and intensities of the bands do not depend very much on the conformation.

Einarsrud et al. [18] calculated only IR values for the C_i ion, and predicted band values considerably higher in frequency than our values, but their spectrum looked much like our spectra. When it comes to comparisons of calculated and observed spectral values, Einarsrud et al. [14, 15, 17, 18] presented FT-infrared reflection spectra of a metastable melt at 200 °C with the composition “ $\text{NaAl}_2\text{OCl}_5$ ”, assumed to contain the $[\text{Al}_4\text{O}_2\text{Cl}_{10}]^{2-}$ ion. After reshaping their spectra into a format that compared with our calculations, the result looked as in Figure 3. Their observed bands at ~ 800 , ~ 681 , ~ 558 and ~ 493 cm^{-1} looked quite the same as our calculated bands at 770, 675, 561 and 496 cm^{-1} . These bands according to the calculations arise from movements of mainly the two O^{2-} ions: mainly Al-O stretching along the long axis of the ion (770 cm^{-1}) and in the molecular plane (675 cm^{-1}) and out of the plane (561 cm^{-1}) and paral-

Table 3. Calculated vibrational spectra for the $[\text{Al}_4\text{O}_2\text{Cl}_{10}]^{2-}$ ion in its two conformations and some experimental results. Modes in bold are shown in Figure 4.

	Wavenumber shifts (cm^{-1})		IR intensities (km/mol)		IR calculated ^a (cm^{-1}) [18]	IR observed ^{a,b} (cm^{-1}) [18]	Raman activity ($\text{\AA}^4/\text{AMU}$)		Depolarization ratios		Vibrational assignment ^{c,d}
	C_s	C_i	C_s	C_i			C_s	C_i	C_s	C_i	
1	8.0	9.0	0.0	0.004			0.001	0.0	0.75	0.75	AlCl ₃ rotations
2	12.1	12.0	0.002	0.0			0.001	0.004	0.75	0.75	AlCl ₃ rotations
3	22.7	21.0	0.02	0.01			0.001	0.0	0.52	0.73	AlCl ₃ rockings oopl
4	40.8	39.6	0.1	0.1			0.0003	0.0	0.75	0.72	AlCl ₃ rockings ipl
5	52.1	51.3	0.4	0.4			0.004	0.0	0.01	0.75	AlCl ₃ rockings oopl
6	53.0	54.2	0.01	0.0			0.21	0.28	0.75	0.75	Al ₂ O ₂ Cl ₄ core rocking
7	54.3	61.2	0.0001	0.0			0.07	0.11	0.75	0.75	Al ₂ O ₂ Cl ₄ core rocking + Cl angle bend
8	72.3	68.1	0.0	0.01			0.004	0.0	0.75	0.65	Cl angle bend
9	79.2	79.1	0.05	0.0			2.7	2.6	0.75	0.75	Cl angle bend
10	89.3	90.1	0.0	0.0			2.2	2.4	0.75	0.75	Cl angle bend
11	95.8	97.9	0.09	0.0			0.52	0.81	0.72	0.69	Umbrella iph
12	100.1	100.6	0.002	0.07			0.06	0.0	0.75	0.61	Cl angle bend
13	100.8	101.5	0.01	1.5			0.64	0.0	0.75	0.70	Cl angle bend
14	104.1	102.4	1.4	0.018			0.17	0.0	0.65	0.75	Cl angle bend
15	113.1	112.2	0.08	0.0			1.3	1.1	0.63	0.62	Cl angle bend
16	138.3	139.1	0.02	0.0			1.9	2.1	0.75	0.75	Al ₂ oopl def
17	148.2	149.4	3.2	0.0			0.008	2.7	0.75	0.75	Al ₁ -O wagging
18	149.8	150.6	15	15	146 m		0.71	0.0	0.75	0.75	Cl angle bend
19	152.5	152.7	0.0	0.0			0.4	2.3	0.75	0.75	Cl angle bend
20	163.6	163.1	3.3	7.9			2.67	0.0	0.75	0.74	Cl angle bend
21	177.2	178.5	97	96.5	176 s	183 w	0.06	0.0	0.75	0.73	Cl umbrella bend
22	187.6	187.1	0.03	0.034			1.25	0.0	0.75	0.75	Cl angle bend + Al ₂ Cl ₂ str
23	261.7	261.4	0.13	0.0			1.6	1.9	0.23	0.26	O-O dist str + umbrella iph
24	281.1	281.8	0.0	0.0			0.21	0.46	0.75	0.75	Al ₂ O ₂ sq twist ipl
25	290.6	286.4	0.01	0.0			0.04	10.9	0.71	0.04	O-O oopl bend + breathing
26	291.8		0.008				25.3		0.03		breathing
		298.4		0.0				15.0		0.03	O-O oopl bend + breathing
27	330.2	326.8	68.3	55.1	359 s	341 w	0.004	0.0	0.75	0.43	Al-Cl str
28	348.3	348.3	2.6	15.1	392 vw	384 vw	0.3	0.0	0.05	0.02	O-O oopl iph bend
29	411.7	412.4	54	55	439 s	423 w	0.02	0.0	0.75	0.43	Al ₂ Cl ₂ ooph sym str
30	420.4	420.4	3.3	0.0			3.2	3.2	0.05	0.05	O-O dist str + umbrella
31	491.2	488.9	157	135	519 s		2.3	0.0	0.75	0.73	Al ₁ inph oopl bend
32	491.9	494.0	13.8	0.002			1.6	3.8	0.75	0.74	Al ₁ ooph oopl bend
33	496.2	496.0	193	193	528 s	493 s,br	0.86	0.001	0.75	0.75	Al ₁ iph ipl bend
34	496.9	496.8	0.1	0.04			2.55	3.7	0.75	0.75	Al ₁ ooph ipl bend
35	510.9	511.6	25.6	59	535 w		0.019	0.0	0.75	0.67	Al ₁ -O asym str
36	520.8	520.7	0.007	0.0	568 m		3.4	3.3	0.75	0.75	Al ₂ ooph oopl str
37	560.8		0.1		594 vs	558 s	1.24		0.75		Al ₂ -O asym ipl str
		561.2		564				0.0		0.32	Al ₁ + Al ₂ oopl iph bend
38	561.2		556		629 m		0.25		0.01		Al ₁ + Al ₂ oopl iph bend
		563.5		0.002				1.17		0.75	Al ₂ -O asym ipl str
39	612.4	611.6	4	0.0002			3.8	3.8	0.22	0.23	Al breathing
40	673.6	675.1	733	735	780 vs	681 s	0.002	0.0	0.75	0.39	Al ₂ -O ipl asym str
41	770.0	769.6	983	997	893 vs	800 vs	0.01	0.0	0.75	0.17	Al ₁ -O ooph asym str
42	863.5	862.7	11	0.0002			1.1	1.1	0.13	0.14	Al ₁ -O iph sym str

^a m, medium; s, strong; v, very; w, weak; br, broad. ^b For NaAl₂OCl₅ liquid [18]. ^c Al1 denotes the aluminum that only is coordinated to one oxygen atom, and Al2 is the one coordinated to two oxygen atoms. ^d asym, antisymmetric; bend, bending; def, deformation; dist, nonbounded distance; iph, in phase; ipl, in plane; oopl, out of plane; ooph, out of phase; sq, square; str, stretching; sym, symmetric; twist, twisting.

labeled to the plane (496 cm^{-1}), as depicted schematically in Figure 4.

IR spectra of NaAlCl₄ melts with assumed oxide species, formed by addition of AlCl₃ · 6H₂O have also

been studied by Mamantov et al. [5, 30, 46]. Infrared absorption bands assignable to oxide species (at ~ 840 and $\sim 720 \text{ cm}^{-1}$) were observed in addition to those from the $[\text{AlCl}_4]^-$ ion (mainly a strong absorption

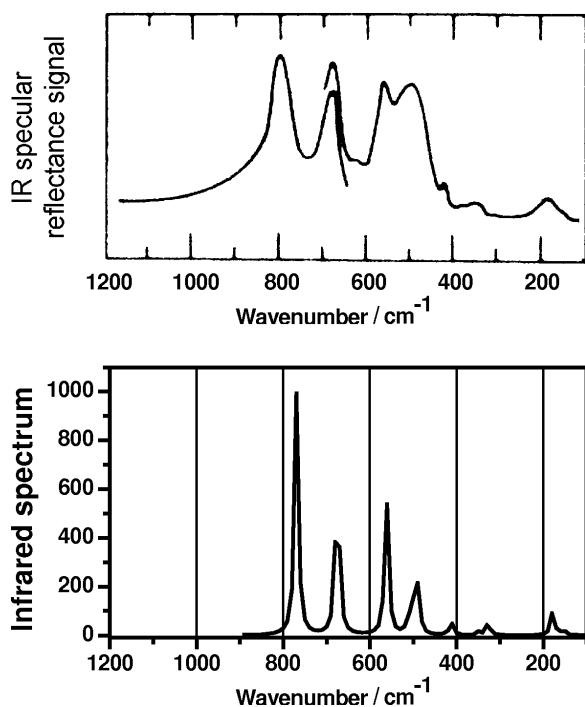


Fig. 3. Comparison between (top) a reshaped experimental FT-infrared specular reflectance spectrum measured from a metastable “ $\text{NaAl}_2\text{OCl}_5$ ” melt at $200\text{ }^\circ\text{C}$ [14, 15, 17, 18] and (bottom) our calculated IR spectrum for an $[\text{Al}_4\text{O}_2\text{Cl}_{10}]^{2-}$ ion in C_i conformation.

band at $\sim 480\text{ cm}^{-1}$). These bands compare reasonably well to our results, noting that the $[\text{AlCl}_4]^-$ *ab initio* vibrational prediction gave a ν_3 band at 484 cm^{-1} . IR spectral bands at ca. 800 and 680 cm^{-1} were also seen in NaCl saturated NaAlCl_4 melts at $200\text{ }^\circ\text{C}$ – assumed to be pure [3] – and the bands were erroneously assigned to overtones [6]. The IR bands could be removed by treatments with phosgene [30] or carbon tetrachloride [31].

With respect to the Raman spectra, very little information has unfortunately been published. No Raman spectrum of any neat $[\text{Al}_4\text{O}_2\text{Cl}_{10}]^{2-}$ melt was obtained. However, we have previously recorded Raman spectra of melts that probably contained the $[\text{Al}_4\text{O}_2\text{Cl}_{10}]^{2-}$ ion in dilution [8]. The melts were obtained from zone-refined clear CsAlCl_4 crystals with additions of CsCl and either Cs_2O or AlOCl . The neat melt showed the four characteristic Raman bands of $[\text{AlCl}_4]^-$, and for the melts with oxide additions an additional definitive band at $\sim 265\text{ cm}^{-1}$ was visible, as shown in Figure 5. These melts were not very stable; on standing at $T > 430\text{ }^\circ\text{C}$, the oxide signal grad-

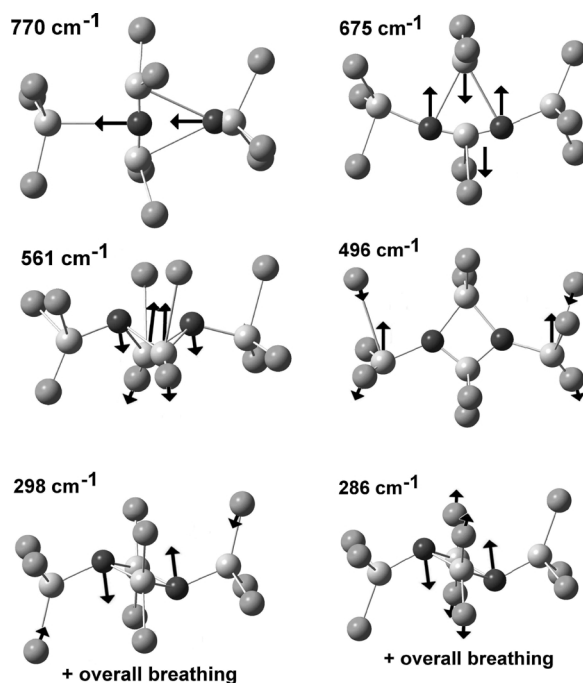


Fig. 4. Displacement vectors for the vibrational modes giving rise to the most characteristic IR and Raman bands of the $[\text{Al}_4\text{O}_2\text{Cl}_{10}]^{2-}$ ion in C_i conformation.

ually decreased and an AlOCl precipitate came out of the melts, that at most contained oxide on the order of $0.1\text{--}0.4\text{ mol L}^{-1}$. The experimental spectra are reproduced in the inset, and also shown are the calculated Raman spectra of the solvent $[\text{AlCl}_4]^-$ ion and the assumed $[\text{Al}_4\text{O}_2\text{Cl}_{10}]^{2-}$ ion in the C_i conformation. The calculated wavenumber shifts and the intensity data are given in Table 3. The strongest Raman bands were calculated for the modes 25 and 26, positioned at ca. 298 and 286 cm^{-1} (polarized) for the C_i conformation (see also Fig. 4). For the $[\text{AlCl}_4]^-$ symmetric stretching mode the Raman band was calculated at 333 or 353 cm^{-1} (Table 1) to compare with the observed value of about 345 cm^{-1} [8, 72]. The observed polarization behaviour was sufficiently conclusive to help establishing the assignment. We note a remarkable agreement, taking into account the limitations in the model, and it seems reasonable to assign the band seen at about 265 cm^{-1} in CsAlCl_4 at $430\text{ }^\circ\text{C}$ as due to the $[\text{Al}_4\text{O}_2\text{Cl}_{10}]^{2-}$ species. This oxochloroaluminate band has previously probably been observed by Torsi et al. in their Raman spectra of molten NaAlCl_4 [73], but they explained it as a difference combination band.

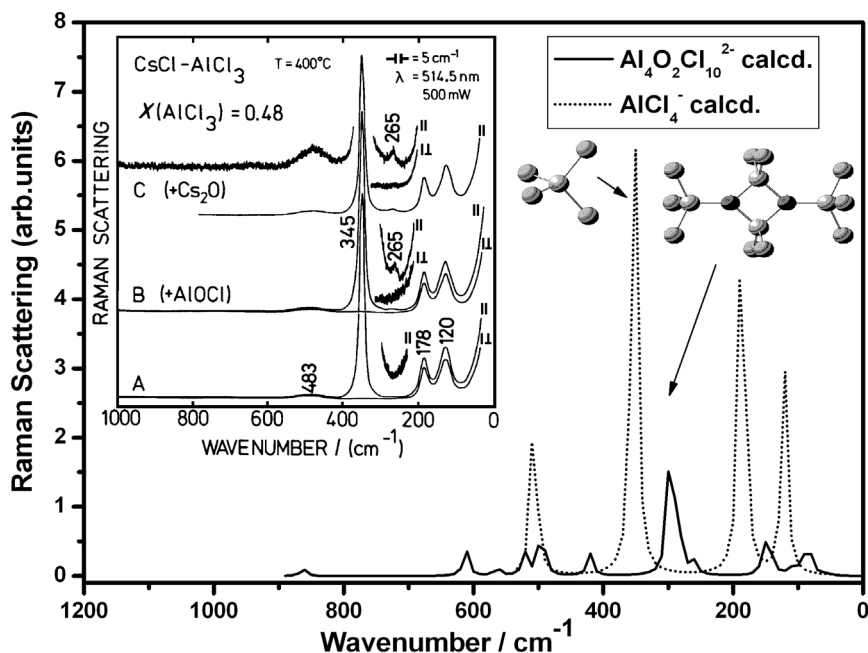


Fig. 5. Comparison between reshaped experimental Raman spectra of water-clear zone-refined CsCl-AlCl_3 melts with oxygen contaminations (insert) and spectra calculated for the $[\text{AlCl}_4]^-$ ion (dotted curve) and the $[\text{Al}_4\text{O}_2\text{Cl}_{10}]^{2-}$ ion in C_i conformation (full curve). The experimental data are from [8].

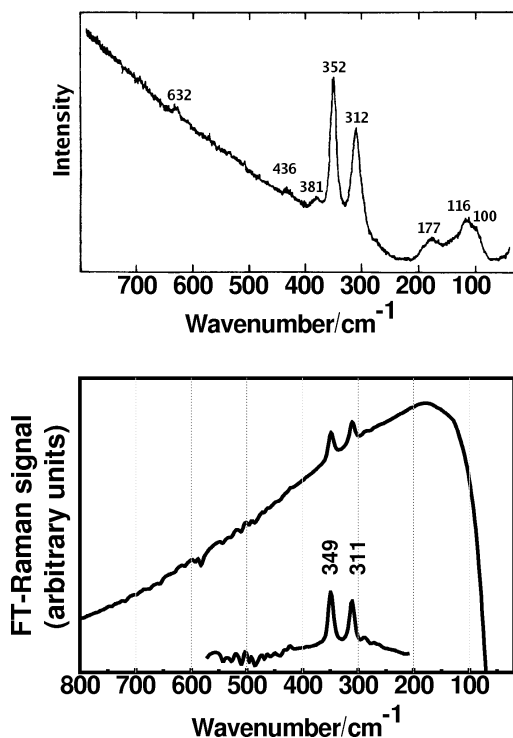


Fig. 6. Comparison between a reshaped experimental Raman spectrum of molten “ $\text{NaAl}_2\text{OCl}_5$ ”-50% NaAl_2Cl_7 mixture (upper) from Einarsrud’s thesis [15] and spectra recorded for our supposed $\text{Ag}_2[\text{Al}_4\text{O}_2\text{Cl}_{10}]\text{-AgCl-AlCl}_3$ mixture at room temperature (lower curves).

Further two pieces of information in this respect may be mentioned: in her thesis [15] Einarsrud has shown a Raman spectrum of the molten “ $\text{NaAl}_2\text{OCl}_5$ ”-50% NaAl_2Cl_7 mixture, and we have recorded our supposed $\text{Ag}_2[\text{Al}_4\text{O}_2\text{Cl}_{10}]\text{-AgAlCl}_4$ mixture at room temperature. The results are given in Figure 6. These spectra were difficult to obtain due to strong fluorescence. They show the strongest modes of $[\text{AlCl}_4]^-$ ($\sim 352\text{ cm}^{-1}$) and $[\text{Al}_2\text{Cl}_7]^-$ ($\sim 312\text{ cm}^{-1}$) [2]. No indication of any $[\text{Al}_4\text{O}_2\text{Cl}_{10}]^{2-}$ was seen.

3.3. Other Oxochloroaluminates

As mentioned, a number of other ions might be postulated to exist. It is certain that practically no free oxide ion, O^{2-} , is present in any chloroaluminate melt, because O^{2-} would react, coordinating to aluminum(III) or replacing chloride, forming eventually $[\text{Al}_2\text{OCl}_6]^{2-}$ (= AlCl_4^- solvated by AlOCl_2^-), $[\text{Al}_3\text{OCl}_8]^-$, $[\text{Al}_2\text{O}_2\text{Cl}_4]^{2-}$, $[\text{Al}_3\text{O}_2\text{Cl}_6]^-$ and perhaps others. We have calculated in similar ways as for $[\text{Al}_4\text{O}_2\text{Cl}_{10}]^{2-}$ RHF equilibrium structures with the basis set 6-31+G(p,d) and vibrational spectra to see if any of these ions may constitute a better candidate for the oxide-bearing complex in the $[\text{AlCl}_4]^-$ melts than $[\text{Al}_4\text{O}_2\text{Cl}_{10}]^{2-}$. As discussed below we found no better candidate. The calculated IR and Raman spectra are summarized in Figures 7 and 8.

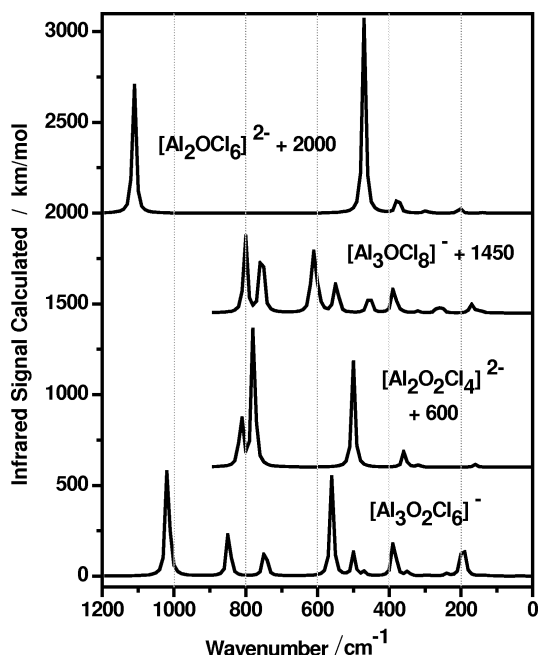


Fig. 7. Calculated IR spectra of the indicated ions, shifted as shown.

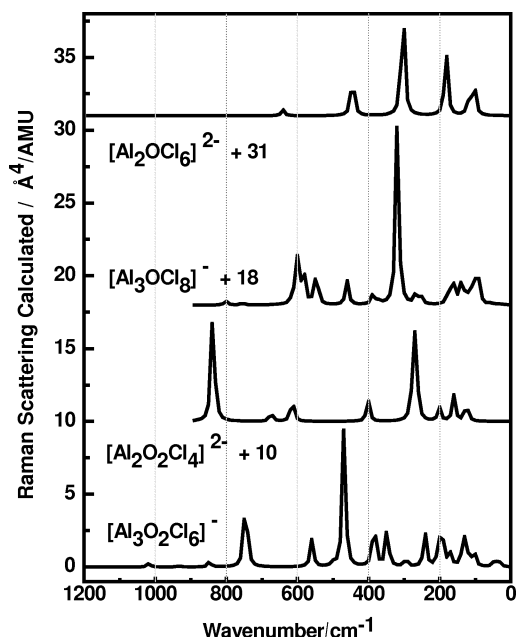


Fig. 8. Calculated Raman spectra of the indicated ions, shifted as shown.

The $[\text{Al}_2\text{OCl}_6]^{2-}$ ion would be expected structurally to consist of two tetrahedrons connected through a bridging oxygen atom. Previously, theoretical *ab initio* MO quantum mechanical calculations done by

Picard et al. [64] of the analogous $[\text{Al}_2\text{OF}_6]^{2-}$ ion have given a linear Al-O-Al bonding system of staggered AlF_3 -groups (approximate D_{3d} symmetry), and we also found the linear Al-O-Al geometry [63]. Our new results for the $[\text{Al}_2\text{OCl}_6]^{2-}$ ion (minimum energy = -3316.23637241 A. U.) again confirmed the convergence to a D_{3d} symmetry with an almost linear Al-O-Al bond, even though we expected a bent Al-O-Al skeleton. The chloride atoms were staggered, and bonds of short but reasonable lengths were found (Al-O = 1.688 and Al-Cl = 2.212 Å). The reason why linear Al-O-Al skeletons were found is not known. Simple valence bond electron counting would give two lone pairs on the oxygen atom which would tend to bend the skeleton. One explanation may be that aluminium atom orbitals could accommodate some of the charge diminishing the electrostatic repulsion between the halogen atoms at both ends of the ion. Another explanation might be that the basis sets for aluminium are not good enough. The calculated spectra of $[\text{Al}_2\text{OCl}_6]^{2-}$ showed IR bands (in Fig. 7, top) at 1111 (s, Al-O-Al asym str), 470 (vs, Al-O-Al degenerate bend + Al-Cl str), 375 (w, AlCl_3 sym str ooph), 297 (vw, Al-O-Al degenerate bend), 203 (vw, AlCl_3 umbrella bend ooph) and 37 cm^{-1} (vww, AlCl_3 bend). Raman bands (in Fig. 8, top) were found at 641 (w, O-Al-O sym str), 445 cm^{-1} (m, Al-Cl degenerate str), 303 cm^{-1} (vs, Al-Cl breathing sym str), 182 cm^{-1} (s, AlCl degenerate sym bend), 121 cm^{-1} (m, AlCl_3 sym bend umbrella iph), 104 cm^{-1} (m, AlCl degenerate sym bend iph). Codes for the intensities and assignments are given in a footnote in Table 3. The spectra do not agree with the spectral observations (Figs. 3 and 5) and with the cryoscopic results (presence of dioxo species [4]). In conclusion, the $[\text{Al}_2\text{OCl}_6]^{2-}$ ion does not seem to be present in the experiments.

The unique $[\text{Al}_3\text{OCl}_8]^-$ ion, found by Thewalt and Stollmaier [44], has a structure consisting of a central oxygen atom, surrounded by three aluminium atoms in a triangle and eight chloride atoms (Fig. 9, left). The Al-O bonds (of length 1.76 Å) reached to one AlCl_2 -group (Al1-Cl bonds of 2.07 Å) and two AlCl_3 -groups (Al2-Cl bonds of 2.06–2.09 Å). When performing RHF optimization calculations we got good convergence to a structure with minimum energy = -4477.36220037 A.U. and reasonable parameters (Al-O = 1.795, 1.832, Al-Cl = 2.11, 2.14 and 2.31 Å). The ion geometry was slightly different from the X-ray structure, in having one AlCl_3 group and two AlCl_2 groups coordinated to the oxygen atom and one

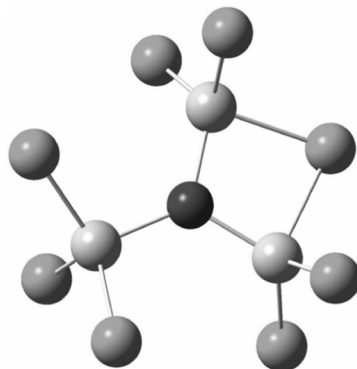
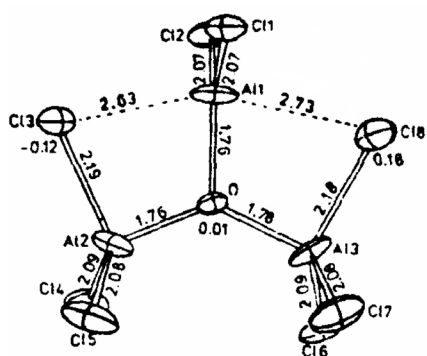


Fig. 9. The $[\text{Al}_3\text{OCl}_8]^{2-}$ ion structure by Thewalt and Stollmaier [44] and by RHF optimization (minimum energy = -4477.36220037 A.U. and bond distances Al-O = 1.832 and 1.795 and Al-Cl = 2.11, 2.14 and 2.31 Å). The calculated geometry differed from the X-ray structure in having one AlCl_3 group and two AlCl_2 groups coordinated to the oxygen atom and with one chloride bridging between aluminum.

chloride atom bridging between two aluminium ions (see Fig. 9). The spectra calculated for the $[\text{Al}_3\text{OCl}_8]^{2-}$ ion (in Fig. 7 for IR and in Fig. 8 for Raman) had the most pronounced IR bands at 801 (vs, Al-O str), 755 (s, Al-O asym str), 613 (s, Al-O str + OAl_2 bend), 600 (m, O- Al_3 sym str), 551 (m, Al-Cl str), 544 (m, Al-Cl str), 455 (m, AlCl_2 sym str ooph), 387 (m, Al-Cl str), 265 (w, Al-Cl_{bridge} asym str), 252 (w, Al-Cl_{bridge} str), and 171 cm^{-1} (w, Cl bend) and Raman bands at 600 (s, O-Al sym str), 582 (m, Al-Cl str), 551 (m, Al-Cl str), 544 (m, Al-Cl str), 460 (m, O-Al str + OAl_2 bend), 319 (vs, OAl_3 sym str breathing), 266 (vw, OAl_2 bend), 160 (w, AlCl bend), 136 (vw, AlCl bend), 102 (w, AlCl bend) and 90 cm^{-1} (w, AlCl bend). The spectra do not perfectly agree with the spectral observations and the formula with one oxygen atom conflicts the cryoscopic results that required the presence of dioxo species [4]. We conclude that the $[\text{Al}_3\text{OCl}_8]^{2-}$ ion probably has not been seen in the mentioned experiments (see Figs. 3 and 5).

An assumed $[\text{Al}_2\text{O}_2\text{Cl}_4]^{2-}$ ion, when minimized using 6-31+G(d,p) basis sets, converged to a minimum (RHF energy = -2472.00067356 A. U.) with a reasonable geometry (bond lengths Al-O = 1.75 and Al-Cl 2.24 Å), see Fig. 10, left. The minimized ion showed calculated spectra as depicted in Figs. 7 and 8. The bands were positioned in the IR spectrum at 813 (m, Al_2O_2 def), 778 (s, Al_2O_2 def + Cl angle bend), 500 (s, Al_2O_2 def), 358 (m, AlCl_2 ooph sym str), 317 (vw, AlCl str), 163 (vw, AlCl_2 ooph bend) and 159 cm^{-1} (vw, AlCl bend) and in the Raman spectrum at 837 (s, Al_2O_2 core breathing), 674 (w, Al-O asym str), 614 (m, Al⁺-Al str), 401 (m, Al-Cl str), 272 (s, Al-Cl sym str), 263 (w, AlCl_2 wag), 201 (m, O_2 twist around Al-Al axis), 160 (m, Al_2 twist around O-O axis) and 125 cm^{-1} (m, AlCl_2 sym angle bend). The spectra did not at all agree with the observations but fitted the

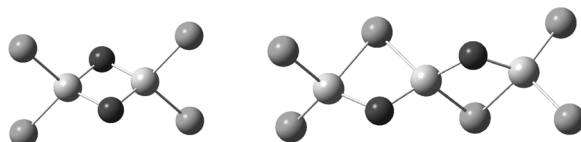


Fig. 10. The $[\text{Al}_2\text{O}_2\text{Cl}_4]^{2-}$ ion structure (left) and the $[\text{Al}_3\text{O}_2\text{Cl}_6]^{2-}$ ion structure (right) as determined by *ab initio* restricted Hartree-Fock 6-31+G(d,p) optimizations.

cryoscopic results (presence of dioxo species [4]). Especially the strong IR and Raman signals, respectively, at 500 and 887 cm^{-1} were not seen (see Figs. 3 and 5). Therefore the $[\text{Al}_2\text{O}_2\text{Cl}_4]^{2-}$ ion cannot claim any existence in the experiments.

Finally we calculated on the assumed ion $[\text{Al}_3\text{O}_2\text{Cl}_6]^{2-}$. The *ab initio* Hartree-Fock 6-31+G(d,p) optimized model structure had an energy of -3633.16481593 A. U. and reasonable structural parameters (bond lengths Al-O = 1.70 Å, Al-Cl = 2.13, 2.31 and 2.42 Å), see Fig. 10, right. The calculated spectra are shown at the bottom of Fig. 7 (IR) and Fig. 8 (Raman). The bands were positioned, in the IR spectrum at 1017 (s, Al-O str), 847 (m, Al-O str), 745 (m, Al-O def), 559 (s, AlCl str), 499 (w, OAl_2 bend), 387 (m, OAl_2 bend + AlCl str) and 196 cm^{-1} (m, AlCl str), and in the Raman spectrum at 847 (vw, Al_2O_2 core str), 746 (s, Al-O sym str), 560 (m, AlCl_2 str), 469 (s, Al-Cl str + OAl_2 bend), 388 (m, Al-Cl sym str), 348 (m, AlCl_2 str + OAl_2 bend), 241 (m, Al-Cl str), and several mixed stretchings and bendings were seen in the 100–200 cm^{-1} range. Also these spectra do not at all agree with the observations (especially the strong IR and Raman signals, respectively, at 1017 and 469 cm^{-1} , see Figs. 3 and 5). Although the cryoscopic results [4] (presence of dioxo species) were in accord with the formula, we conclude that the $[\text{Al}_3\text{O}_2\text{Cl}_6]^{2-}$ ion cannot be present in the experimental melts.

4. Conclusion

Calculations using the Gaussian 03W program generally converged to the presumed structures, and subsequent calculations of spectra made it possible – by comparison with observations – to determine the $[\text{Al}_4\text{O}_2\text{Cl}_{10}]^{2-}$ ion as the most probable oxochloroaluminate ion in tetrachloroaluminate melt environments. Its spectra have been predicted and assigned, and the strength of the quantum chemical calculations has been shown once again.

Acknowledgement

I wish to thank Profs. Irene Shim (DTU, Lyngby, Denmark) and Terje Østvold (Trondheim University) for help initiating this work. I am grateful to DTU for travel grants and wish to acknowledge helpful discussions with Susanne B. Hansen (Sisimiut, Greenland), Niels J. Bjerrum (DTU), Bernard Gilbert (UdL, Liege, Belgium), and Søren Barsberg (DFU, Copenhagen, Denmark).

- [1] M. J. Frisch, G. W. Trucks, H. B. Schlegel, G. E. Scuseria, M. A. Robb, J. R. Cheeseman, J. A. Montgomery Jr., T. Vreven, K. N. Kudin, J. C. Burant, J. M. Millam, S. S. Iyengar, J. Tomasi, V. Barone, B. Menonucci, M. Cossi, G. Scalmani, N. Rega, G. A. Petersson, H. Nakatsuji, M. Hada, M. Ehara, K. Toyota, R. Fukuda, J. Hasegawa, M. Ishida, T. Nakajima, Y. Honda, O. Kitao, H. Nakai, M. Klene, X. Li, J. E. Knox, H. P. Hratchian, J. B. Cross, C. Adamo, J. Jaramillo, R. Gomperts, R. E. Stratmann, O. Yazyev, A. J. Austin, R. Cammi, C. Pomelli, J. W. Ochterski, P. Y. Ayala, K. Morokuma, G. A. Voth, P. Salvador, J. J. Dannenberg, V. G. Zakrzewski, S. Dapprich, A. D. Daniels, M. C. Strain, O. Farkas, D. K. Malick, A. D. Rabuck, K. Raghavachari, J. B. Foresman, J. V. Ortiz, Q. Cui, A. G. Baboul, S. Clifford, J. Cioslowski, B. B. Stefanov, G. Liu, A. Liashenko, P. Piskorz, I. Komaromi, R. L. Martin, D. J. Fox, T. Keith, M. A. Al-Laham, C. Y. Peng, A. Nanayakkara, M. Challacombe, P. M. W. Gill, B. Johnson, W. Chen, M. W. Wong, C. Gonzalez, and J. A. Pople, Gaussian 03W, Revision B.04, Gaussian, Inc., Pittsburgh 2003.
- [2] E. Rytter, H. A. Øye, S. J. Cyvin, B. N. Cyvin, and P. Klæboe, *J. Inorg. Nucl. Chem.* **35**, 1185 (1973).
- [3] N. R. Smyrl, G. Mamantov, and L. E. McCurry, *J. Inorg. Nucl. Chem.* **40**, 1489 (1978).
- [4] R. W. Berg, H. A. Hjuler, and N. J. Bjerrum, *Inorg. Chem.* **23**, 557 (1984).
- [5] C. B. Mamantov, T. M. Laher, R. P. Walton, and G. Mamantov, *Light Met.*, 519 (1985).
- [6] J. Hvistendahl, P. Klæboe, E. Rytter, and H. A. Øye, *Inorg. Chem.* **23**, 706 (1984).
- [7] R. W. Berg, H. A. Hjuler, and N. J. Bjerrum, *Inorg. Chem.* **24**, 4506 (1985).
- [8] R. W. Berg and T. Østvold, *Acta Chem. Scand. A* **40**, 445 (1986).
- [9] R. W. Berg, T. L. Lauridsen, T. Østvold, H. A. Hjuler, J. H. von Barner, and N. J. Bjerrum, *Acta Chem. Scand. A* **40**, 646 (1986).
- [10] J. H. von Barner, N. J. Bjerrum, and R. W. Berg, *Proc. Electrochem. Soc.* **86-1**, 216 (1986).
- [11] K. Zachariassen, R. W. Berg, N. J. Bjerrum, and J. H. von Barner, *J. Electrochem. Soc.* **134**, 1153 (1987).
- [12] E. Rytter, *Proc. Electrochem. Soc.* **85-2**, 721 (1985).
- [13] E. Rytter, *Proc. Electrochem. Soc.* **86-1**, 275 (1986).
- [14] M.-A. Einarsrud and E. Rytter, *Proc. Electrochem. Soc.* **87-2**, 2038 (1987).
- [15] M.-A. Einarsrud, Thesis, Trondheim University, Norway 1987.
- [16] M.-A. Einarsrud, H. Justnes, E. Rytter, and H. A. Øye, *Polyhedron* **6**, 975 (1987).
- [17] M.-A. Einarsrud and E. Rytter, *Mikrochim. Acta* **2**, 381 (1988).
- [18] M.-A. Einarsrud, E. Rytter, and M. Ystenes, *Vib. Spectrosc.* **1**, 61 (1990).
- [19] B. Gilbert, S. D. Williams, and G. Mamantov, *Inorg. Chem.* **27**, 2359 (1988).
- [20] B. P. Gilbert, R. W. Berg, and N. J. Bjerrum, *Appl. Spectrosc.* **43**, 336 (1989).
- [21] R. J. Gale, B. Gilbert, and R. A. Osteryoung, *Inorg. Chem.* **17**, 2728 (1978).
- [22] R. J. Gale and R. A. Osteryoung, *Inorg. Chem.* **19**, 2240 (1980).
- [23] S. Tait and R. A. Osteryoung, *Inorg. Chem.* **23**, 4352 (1984).
- [24] C. J. Dymek Jr., J. S. Wilkes, M.-A. Einarsrud, and H. A. Øye, *Polyhedron* **7**, 1139 (1988).
- [25] B. Gilbert, J.-P. Pauly, Y. Chauvin, and F. DiMarco-Van Tiggelen, *Electrochem. Soc.* **94-13**, 218 (1994).
- [26] S. Takahashi, L. A. Curtiss, D. Gosztola, N. Koura, and M.-L. Saboungi, *Inorg. Chem.* **34**, 2990 (1995).
- [27] J.-P. Schoebrechts, P. A. Flowers, G. W. Hance, and G. Mamantov, *J. Electrochem. Soc.* **135**, 3057 (1988).
- [28] F. Seon, G. Picard, and B. Tremillon, *Electrochim. Acta* **28**, 209 (1983).
- [29] A. K. Abdul-Sada, A. G. Avent, M. J. Parkington, T. A. Ryan, K. R. Seddon, and T. Welton, *J. Chem. Soc., Chem. Commun.* **1987**, 1643 (1987).
- [30] I.-W. Sun, K. D. Sienerth, and G. Mamantov, *J. Electrochem. Soc.* **138**, 2850 (1991).
- [31] G.-S. Chen, I.-W. Sun, K. D. Sienerth, A. G. Edwards,

- and G. Mamantov, *J. Electrochem. Soc.* **140**, 1523 (1993).
- [32] G. Mamantov, G.-S. Chen, H. Xiao, Y. Yang, and E. Hondrogiannis, *J. Electrochem. Soc.* **142**, 1758 (1995).
- [33] T. A. Zawodzinski Jr. and R. A. Osteryoung, *Proc. Joint Int. Symp. Molten Salts* **87-7**, 406 (1987).
- [34] H. Kurayasu and Y. Inokuma, *Anal. Chem.* **65**, 1210 (1993).
- [35] L. A. Curtiss and M. Blander, *J. Electrochem. Soc.* **131**, 2271 (1984).
- [36] G. Letisse and B. Tremillon, *J. Electroanal. Chem. Interfacial Electrochem.* **17**, 387 (1968).
- [37] B. Tremillon, A. Bermond, and R. Molina, *J. Electroanal. Chem. Interfacial Electrochem.* **74**, 53 (1976).
- [38] J. Robinson, B. Gilbert, and R. A. Osteryoung, *Inorg. Chem.* **16**, 3040 (1977).
- [39] B. Gilbert and R. A. Osteryoung, *J. Am. Chem. Soc.* **100**, 2725 (1978).
- [40] F. Taulelle, C. Piolet, and B. Tremillon, *J. Electroanal. Chem. Interfacial Electrochem.* **134**, 131 (1982).
- [41] G. Mamantov and C. B. Mamantov, US Patent No. 4493784, 4 pp. (1985).
- [42] T. M. Laher, L. E. McCurry, and G. Mamantov, *Anal. Chem.* **57**, 500 (1985).
- [43] R. Fehrmann, J. H. Von Barner, N. J. Bjerrum, and O. F. Nielsen, *Inorg. Chem.* **20**, 1712 (1981).
- [44] U. Thewalt and F. Stollmaier, *Angew. Chem. Int. Ed. Engl.* **21**, 133 (1982); *Angew. Chem.* **94**, 137 (1982); *Angew. Chem. Suppl.*, 209 (1982).
- [45] D. Jentsch, P. G. Jones, E. Schwarzmans, and G. M. Sheldrick, *Acta Crystallogr. C* **39**, 1173 (1983).
- [46] P. A. Flowers and G. Mamantov, *Anal. Chem.* **59**, 1062 (1987).
- [47] E. W. Dewing and J. Thonstad, *Metall. Mater. Trans. B* **28**, 1089 (1997).
- [48] M. H. Brooker, R. W. Berg, J. H. von Barner, and N. J. Bjerrum, *Inorg. Chem.* **39**, 4725 (2000).
- [49] M. H. Brooker, R. W. Berg, J. H. von Barner, and N. J. Bjerrum, *Inorg. Chem.* **39**, 3682 (2000).
- [50] J. Thonstad, *Adv. Molten Salt Chem.* **6**, 73 (1987).
- [51] S. K. Ratkje, *Electrochim. Acta* **21**, 515 (1976).
- [52] A. Sterten, *Electrochim. Acta* **25**, 1673 (1980).
- [53] A. Sterten, K. Hamberg, and I. Maeland, *Acta Chem. Scand. A* **36**, 329 (1982).
- [54] A. Sterten and O. Skar, *Aluminium (Isernhagen, Germany)* **64**, 1051 (1988).
- [55] B. Gilbert, E. Robert, E. Tixhon, J. E. Olsen, and T. Østvold, *Light Met.*, 181 (1995).
- [56] V. Danek, Ø. T. Gustavsen, and T. Østvold, *Can. Metall. Quart.* **39**, 153 (2000).
- [57] T. Førland and S. K. Ratkje, *Acta Chem. Scand.* **27**, 1883 (1973).
- [58] B. Gilbert, T. Foosnaes, and R. Huglen, *PCT/NO99/00250 Int. Appl.* **2000**, (24 Feb.) 17 pp. CAN 132:154729: 133911 (2000).
- [59] E. Robert, J. E. Olsen, B. Gilbert, and T. Østvold, *Acta Chem. Scand.* **51**, 379 (1997).
- [60] E. Robert, J. E. Olsen, V. Danek, E. Tixhon, T. Østvold, and B. Gilbert, *J. Phys. Chem. B* **101**, 9447 (1997).
- [61] E. Robert and B. Gilbert, *Appl. Spectrosc.* **54**, 396 (2000).
- [62] F. Auguste and B. Gilbert, A Study of the Dissociation of Fluoroaluminates in FLiNaK by Raman Spectroscopy, in: *Progress in Molten Salts Chemistry*, Vol. 1 (Eds. R. W. Berg and H. A. Hjuler), Elsevier, Paris 2000, pp. 71–74.
- [63] M. H. Brooker, R. W. Berg, and J. D. C. Craig, *Ab Initio* Calculations on the Structure and Vibrational Spectra of $\text{Al}_2\text{OF}_6^{2-}$ and $\text{B}_2\text{OF}_6^{2-}$ Ions, in: *Progress in Molten Salts Chemistry*, Vol. 1 (Ed. R. W. Berg and H. A. Hjuler), Elsevier, Paris 2000, pp. 111–118.
- [64] G. S. Picard, F. C. Bouyer, M. Leroy, Y. Bertaud, and S. Bouvet, *J. Mol. Struct. (Theochem.)* **368**, 67 (1996).
- [65] L. A. Curtiss and R. Nichols, *Proc. Electrochem. Soc.* **86-1**, 289 (1986).
- [66] M. Ystenes and B. K. Ehrhardt, *J. Mol. Struct. (Theochem.)* **303**, 155 (1994).
- [67] C. W. Bock, M. Trachtman, and G. J. Mains, *J. Phys. Chem.* **98**, 478 (1994).
- [68] G. J. Mains, E. A. Nantsis, and W. R. Carper, *J. Phys. Chem. A* **105**, 4371 (2001).
- [69] A. Y. Timoshkin, A. V. Suvorov, and H. F. Schaefer III, *Russ. J. General Chem. (Translation of Zhurnal Obshchei Khimii)* **68**, 1609 (1998).
- [70] F. Wallart, A. Lorriaux-Rubbens, G. Mairesse, P. Barbier, and J. P. Wignacourt, *J. Raman Spectrosc.* **9**, 55 (1980).
- [71] B. Krebs, H. Greiwing, C. Brendel, F. Taulelle, M. Gaune-Escard, and R. W. Berg, *Inorg. Chem.* **30**, 981 (1991).
- [72] V. A. Narayanan, *J. Raman Spectrosc.* **20**, 77 (1989).
- [73] G. Torsi, G. Mamantov, and G. M. Begun, *Inorg. Nucl. Chem. Lett.* **6**, 553 (1970).